PHYSICAL REVIEW
LETTERS

VOLUME 78 19 MAY 1997 NUMBER 20

Emergence of Interaction Effects in Bose-Einstein Condensation

M. J. Holland, D. S. Jin,* M. L. Chiofalo,† and J. Cooper
JILA, National Institute of Standards and Technology, and Department of Physics, University of Colorado, Boulder, Colorado 80309-0440
(Received 7 November 1996)

We present a quantitative evaluation of the predictions of mean-field theory for describing a Bose-Einstein condensate in a magnetic trap by comparing directly with experimental observations. We study the release energy from ballistic expansion and the cloud density profile as a function of mean-field effects. Significant departure of the cloud shape from both the noninteracting limit and the strongly repulsive limit is observed for our parameters, consistent with theoretical prediction. [S0031-9007(97)03183-9]

PACS numbers: 03.75.Fi, 05.30.Jp, 32.80.Pj

One reason the recent observations of Bose-Einstein condensation in alkali gases [1–3] have generated so much interest is the ability to provide accurate and detailed theory in a quantum degenerate many body system. In these experiments, the average distance between the particles is much larger than the characteristic length scale associated with elastic binary collisions. The gas is dilute and well modeled at zero temperature by mean-field theory for a finite system of weakly interacting bosons [4]. This has allowed direct microscopic calculations of many experimental observables such as the frequencies of elementary excitations, the conditions required for vortex formation, and the effect of finite number and size on the thermodynamics [5,6]. Application of the Gross-Pitaevskii equations to this problem showed qualitative agreement with the spatial features of the experimentally observed condensate component [7]. As one would expect, the noncondensate atoms showed a contrasting spatial distribution consistent with the equipartition theorem [8]. In the case of superfluid helium, where the density is much higher, fluctuations about the mean field even at zero temperature make a similar microscopic description of the condensate more complicated.

In this Letter, we present measurements of the release energy of a Bose-Einstein condensate and the density distribution after ballistic expansion and make direct comparison with theory. For our parameters, kinetic energy effects in the condensate are important and the Thomas-Fermi approximation (neglecting the particle kinetic energy) is not valid. The significance of our quantitative comparisons between experiment and theory is that there are effectively no fitting parameters. The few parameters required by the theory can easily be measured independently of the energy and shape studies performed here.

The numerical prediction of time-dependent phenomena in these systems using mean-field theory represents a significant computational problem. The experiments have only one axis of rotational symmetry and therefore two-dimensional wave functions at least must be stored. The problem is made difficult by the mean-field nonlinearity, the singularity at the radial origin, and the requirement to model the ballistic expansion where the multidimensional wave function grows to many times its original size. An efficient method has been developed to solve this problem over a wide range of interaction strengths. The starting point is the time-dependent Gross-Pitaevskii equation giving the evolution of the condensate wave function $\psi(\boldsymbol{r}, t)$ at the point $\boldsymbol{r} \equiv (x, y, z)$

$$i\hbar \frac{\partial \psi(\boldsymbol{r}, t)}{\partial t} = -\frac{\hbar^2}{2m}\nabla^2 \psi(\boldsymbol{r}, t) + V(\boldsymbol{r})\psi(\boldsymbol{r}, t) + NU_0 |\psi(\boldsymbol{r}, t)|^2 \psi(\boldsymbol{r}, t), \quad (1)$$

where m is the mass of the atom. The confining potential in the experiment is harmonic, $V(\boldsymbol{r}) = \frac{1}{2}m\omega^2(x^2 + y^2 + \epsilon z^2)$, where $\omega = 2\pi\nu$ is given in terms of the horizontal oscillation frequency ν. The anisotropy parameter for our

field geometry is $\epsilon = 8$ which is the ratio of the vertical (z direction) and horizontal spring constants. The last term in Eq. (1) is the mean field which is proportional to the number of condensate atoms N, the scattering length a through $U_0 \equiv 4\pi\hbar^2 a/m$, and the wave function density which is normalized $\int d^3r|\psi(\mathbf{r},t)|^2 = 1$.

Because of the vertical axis of rotational symmetry in $V(\mathbf{r})$, we use as coordinates only the height z and the distance from the vertical axis $r = \sqrt{x^2 + y^2}$. We also scale lengths to the natural size of the harmonic oscillator ground state $l = \sqrt{\hbar/(2m\omega)}$ by introducing dimensionless variables $\rho \equiv r/l$, $\zeta \equiv z/l$, and $\alpha \equiv a/l$. The wave function is defined only for ρ positive and for this reason it is usually easiest to treat numerically if the calculated wave function is zero at $\rho = 0$. We therefore define a computed wave function $\varphi(\rho,\zeta,t) \equiv \sqrt{l}\, z\rho\psi(\rho,\zeta,t)$. Using $\tau \equiv \omega t$, the dimensionless form of Eq. (1) is

$$i\frac{\partial\varphi(\rho,\zeta)}{\partial\tau} = \left[-\frac{\partial^2}{\partial\zeta^2} - \frac{\partial^2}{\partial\rho^2} + \frac{1}{\rho}\frac{\partial}{\partial\rho} - \frac{1}{\rho^2} + \frac{1}{4}(\rho^2 + \epsilon\zeta^2) + \frac{8\pi N\alpha|\varphi(\rho,\zeta)|^2}{\rho^2}\right] \times \varphi(\rho,\zeta), \quad (2)$$

where $2\pi\int\rho^{-1}|\varphi(\rho,\zeta)|^2 d\rho\, d\zeta = 1$ is the normalization condition on $\varphi(\rho,\zeta)$.

We numerically evaluate Eq. (2) for the experimental parameters using an alternating-direction implicit (ADI) method which is based on finite differencing in each dimension to derive the derivatives [9]. Although implementing this for the derivative term arising from the vertical kinetic energy $\partial^2/\partial\zeta^2$ is straightforward, it is nontrivial to treat $\rho = 0$ in the terms arising from the horizontal kinetic energy; $\partial^2/\partial\rho^2$, $1/\rho\,\partial/\partial\rho$, and $1/\rho^2$. A number of the current Bose-Einstein condensation experiments have cylindrical geometry and are therefore described by equations of this form, so that a procedure to treat carefully the region near the symmetry axis is important. Sampling the wave function at a grid of points spaced Δ apart defines a discretized wave function $\varphi_{j,s} = \varphi(j\Delta, s\Delta)$ for integers j and s. The difficulty in calculating the radial kinetic energy is that second-order central finite differencing for the horizontal kinetic energy terms does not give a good numerical approximation to the derivative for radial points j close to 0. In our approach, we numerically approximate these terms at $\rho = j\Delta$ and $\zeta = s\Delta$ by

$$\frac{\partial\varphi(\rho,\zeta)}{\rho\,\partial\rho} \to \beta_j\frac{\varphi_{j+1,s} - \varphi_{j-1,s}}{2j\Delta^2} + (1-\beta_j)\frac{\varphi_{j+2,s} - \varphi_{j,s}}{2(j+1)\Delta^2}, \quad (3)$$

$$\frac{\partial^2\varphi(\rho,\zeta)}{\partial\rho^2} \to \beta_j\frac{\varphi_{j+1,s} - 2\varphi_{j,s} + \varphi_{j-1,s}}{\Delta^2} + (1-\beta_j)\frac{\varphi_{j+2,s} - 2\varphi_{j+1,s} + \varphi_{j,s}}{\Delta^2}.$$

The terms on the right hand side weighted by β_j are central differencing, and those weighted by $1 - \beta_j$ are forward differencing. The parameter β_j is determined analytically by relating the left and right hand sides of these equations for the series expansion of $\varphi(\rho,\zeta) = \sum_n \varphi_n(\zeta)\rho^{n+1}$ near $\rho = 0$. This procedure gives

$$\beta_j = \frac{j(4j+3)}{(2j+1)^2}, \quad (4)$$

which makes the approximation in Eq. (3) exact for $n \leq 2$ and is the optimal choice. Note that β_j tends to unity as j increases so that almost pure central differencing is used at large distances from the vertical axis. In contrast, forward differencing is used exclusively at $j = 0$. We have found this addition to usual ADI numerical methods to be stable and to allow large grid spacing with high numerical accuracy and therefore rapid computation. Any numerical solution of a parabolic equation with cylindrical symmetry may benefit from this approach.

The experimental procedure is to evaporatively cool to an almost pure condensate in which we estimate that the remaining noncondensate atoms represent less than 20% of the sample. We then allow the cloud to ballistically expand by suddenly removing the confining potential. In order to model this, we first find the theoretical self-consistent condensate wave function before expansion. The condensate density profile is dependent on the trap frequency ν which determines the spatial scale l, and the condensate number N, measured from total optical absorption of an imaging pulse. The scattering length a for spin-polarized ^{87}Rb has recently been measured as $110a_0$ (a_0 is the Bohr radius) and is accurate to approximately 9% [10]. The numerical method used to find the self-consistent condensate wave function is to propagate a trial wave function (chosen carefully to be as close as possible to the solution) in imaginary time by replacing i on the left hand side of Eq. (2) by -1, and to renormalize the wave function at each time step. This provides a minimization of the energy by steepest descents and converges rapidly to the ground state solution [6].

We model the ballistic expansion by initializing $\varphi(\rho,\zeta)$ to the self-consistent wave function and evolving the Gross-Pitaevskii equation with the confining potential term removed. During the expansion, the energy components are found by integrating each of the different terms on the right hand side of Eq. (2) over the wave function volume. This gives the axial and radial kinetic energies, E_z and E_r, respectively, the total kinetic energy $E_k = E_z + E_r$, the confining potential energy E_p, and the mean-field interaction energy E_{int}. The volume integrated chemical potential is $\mu = E_k + E_p + E_{\text{int}}$. The time-invariant quantity corresponding to conservation of energy during the expansion is the release energy and is given by $\varepsilon \equiv E_k + E_{\text{int}}/2$. The typical variation of the energy components during expansion is illustrated

in Fig. 1. Because of the repulsive mean field, the total kinetic energy E_k before expansion ($t < 0$) is small and most of the energy is contained in the mean field and potential energy of the particles. At $t = 0$, the harmonic confining potential is removed and E_p from then on is zero. The chemical potential μ decreases during the expansion ($t > 0$) due to the reduction of the mean field. One half of the initial mean-field energy E_{int} is transferred into kinetic energy E_k at large expansion times as illustrated by the time invariance of ε.

In Fig. 2 we show four snapshot images of the numerical density profile as it expands illustrating the self-diffraction of the condensate wave function. The number of condensate atoms and the frequency of the initial trap are the same as for Fig. 1. The wave function is initially confined more strongly in the z direction than in the x direction due to the trap geometry and this translates to a spreading which is larger vertically than horizontally after the confining potential is removed. The numerical model must be able to treat a large change in the spatial scale of the wave function in both dimensions.

It is necessary to find the asymptotic kinetic energy of expanding clouds in the experiment in order to compare the release energy with that predicted by this model. This is done using the experimentally observed density profile as a function of expansion time in the far field regime. In this regime there is maximal correlation between the position of an atom $\boldsymbol{r}$ and its momentum $\boldsymbol{p}$ as constrained by the Schwartz inequality $\langle \boldsymbol{r}^2 \rangle \langle \boldsymbol{p}^2 \rangle \geq |\langle \boldsymbol{r} \cdot \boldsymbol{p} \rangle|^2$. In the expanded cloud, the equality holds and we have $\langle \boldsymbol{r}^2 \rangle \langle \boldsymbol{p}^2 \rangle = \langle \boldsymbol{r} \cdot \boldsymbol{p} + \boldsymbol{p} \cdot \boldsymbol{r} \rangle^2 / 4$ since the commutator $[\boldsymbol{r}, \boldsymbol{p}] = i\hbar$ which is omitted is negligible. The rate of change of the variance $\sigma^2 = \langle \boldsymbol{r}^2 \rangle$ can then be related to the kinetic energy

$$\frac{1}{2} m \left(\frac{\partial \sigma}{\partial t} \right)^2 = \frac{1}{8 m \sigma^2} \langle \boldsymbol{r} \cdot \boldsymbol{p} + \boldsymbol{p} \cdot \boldsymbol{r} \rangle^2 = \frac{\langle \boldsymbol{p}^2 \rangle}{2m} = E_k \,. \tag{5}$$

Consequently, a sequence of experimental measurements of σ at different expansion times is used to derive the kinetic energy. Note that this is a general property where no assumption about the cloud shape has been made.

We determine σ of the experimentally observed density distribution by fitting a simple smooth functional form to the data and finding the moments of this distribution analytically. Our functional form is generated by imposing constraints based on the following properties:

(1) We expect the density distribution at large distances from the center to be well described by a Gaussian tail.

(2) We also expect, in the case of strong interactions, there to be a region in the center of the cloud where the kinetic energy of the atoms can be neglected. In this region the sum of the potential energy due to interactions (proportional to the local density of atoms) and the energy due to the confining potential is required to be spatially uniform.

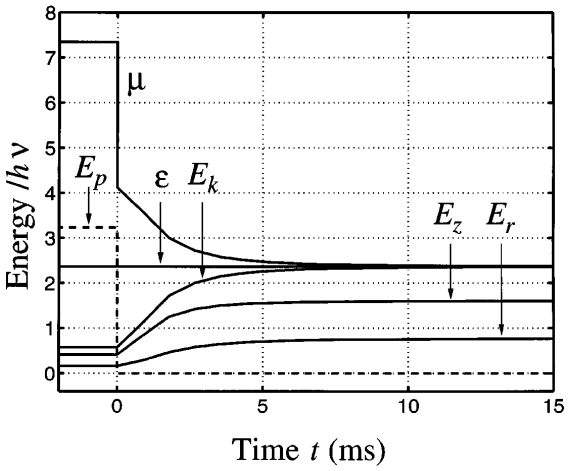

FIG. 1. Theory: Energy components during the expansion of a 4000 atom condensate. The trap frequency was $\nu = 56.25$ Hz and was removed at $t = 0$. Shown are the radial E_r, axial E_z, and total E_k kinetic energies, the potential energy E_p, the release energy ε, and the chemical potential μ.

Taking into account that the camera observes the two-dimensional integrated column density through the cloud, we use the functional form consistent with the above two constraints

$$\mathcal{F} = \begin{cases} H \lambda^{\frac{3}{2}} & \lambda^{\frac{3}{2}} > \kappa \,, \\ H \kappa \exp[-\frac{3}{2}(1 - \lambda/\kappa^{\frac{2}{3}})] & \lambda^{\frac{3}{2}} < \kappa \,, \end{cases} \tag{6}$$

where $\lambda \equiv 1 - x^2/(2\sigma_x^2) - z^2/(2\sigma_z^2)$ parametrizes the elliptical contours. The condition $\lambda^{\frac{3}{2}} > \kappa$ is satisfied in the cloud center, and $\lambda^{\frac{3}{2}} < \kappa$ in the wings of the distribution. The four fitting constants to be determined from the data are the maximum density H, the cloud width in the horizontal and vertical directions, σ_x and σ_z, respectively, and the fraction κ of the maximum

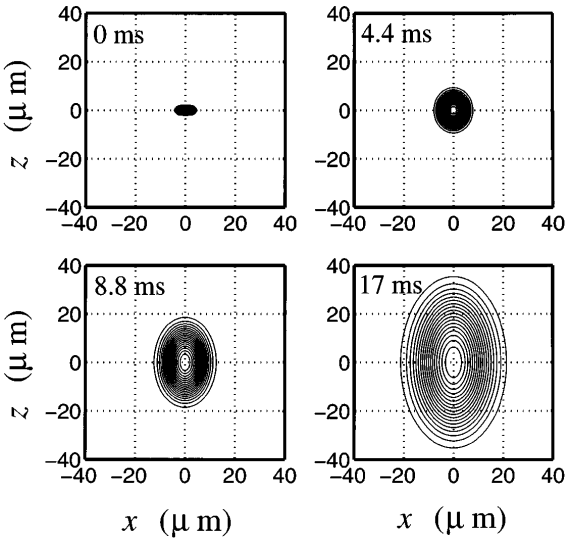

FIG. 2. Theory: Contour images of the wave function density at four times during the expansion of a 4000 atom condensate from a $\nu = 56.25$ Hz trap.

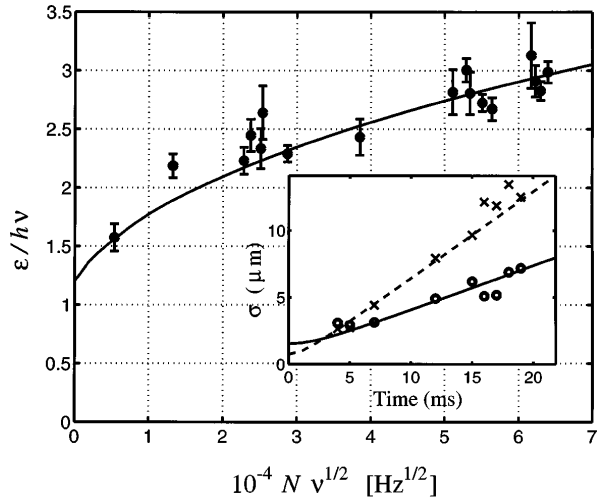

FIG. 3. Comparison of the release energy as a function of interaction strength from mean-field theory (solid line) and the experimental measurements (•). Inset shows experimental widths in the horizontal (∘) and vertical (×) directions against the mean-field predictions (dashed and solid lines) for the data point at $10^{-4}N\nu^{1/2} = 0.53\ \mathrm{Hz}^{1/2}$.

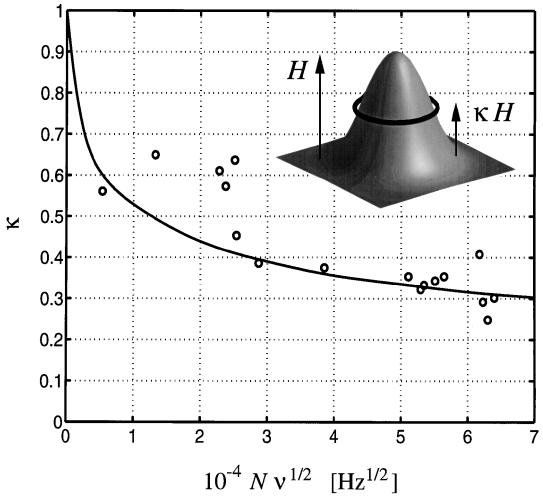

FIG. 4. Comparison of the cloud shape parameter κ as a function of interaction strength for mean-field theory (solid line) and experimental data points (∘).

density at which the Gaussian wings are connected to the central region. Note that on the ellipse $\lambda^{\frac{3}{2}} = \kappa$ the gradient and values of the two parts to the functional form are equal and the density is $H\kappa$. We have found this form to characterize well the density distribution expected theoretically. Choosing optimally H, σ_x, σ_z, and κ to fit this form to the numerically expanded wave function illustrated in Fig. 2 gives a maximum deviation in density of less than 3% over the two-dimensional surface.

In Fig. 3 we present a comparison of the experimentally measured release energy ε [11] with the prediction of Gross-Pitaevskii theory. The relative interaction strength due to mean-field effects is characterized by $N\sqrt{\nu}$. We use this as the dependent variable in order to combine measurements with different condensate numbers and trap frequencies into one graph. The inset shows the time-dependent behavior of the widths of the cloud in the horizontal and vertical directions used to determine experimentally one of the release energy points. Each pair of data points in the inset plot (an × and an ∘ at the same expansion time) represents a separate measurement in which the function given in Eq. (6) is fitted to the observed density profile and both σ_x and σ_z determined. A linear fit to the rate of change of the experimental widths at large expansion times was made (not shown) to determine the asymptotic kinetic energy using Eq. (5). This procedure was repeated for each experimental data point for the release energy (•). The solid line in the main graph and both the solid line and the dashed line in the inset are the predictions of the Gross-Pitaevskii equation which does not contain any fitting parameters to the data set. Our theoretical calculation of the release energy is in agreement with the results reported in Ref. [6] for the unexpanded trap. The theory lines show very good agreement with the experimental data points. The scattering length in the condensate therefore appears to be consistent with that measured in Ref. [10]. A deviation from this value by more than approximately 20% would be inconsistent with our results.

In Fig. 4 we compare the cloud shape parameter κ between theory and experiment, again showing good agreement. The inset shows the typical form of the fitting function with the ellipse representing the boundary between inner and outer parts. At very small values of the interaction strength, κ is close to unity and the cloud shape is approximately Gaussian. At large interactions, κ is smaller and most of the cloud is well approximated by the Thomas-Fermi or strongly repulsive limit. Even for the most strongly interacting clouds, it is necessary to include a significant component of the Gaussian wings.

We thank F. Dalfovo and S. Stringari for providing the results of calculations on the release energy [6]. We thank C. Wieman, E. Cornell, M. Levenson, and the JILA BEC Collaboration for helpful discussions. M. L. C. acknowledges M. Tosi for fruitful discussions and the INFM for financial support. This work was supported by the National Institute for Science and Technology, the National Science Foundation, and the Office of Naval Research.

*Quantum Physics Division, National Institute for Standards and Technology.
†Permanent address: Scuola Normale Superiore and INFM, Pisa, Italy.

[1] M. H. Anderson, J. R. Ensher, M. R. Matthews, C. E. Wieman, and E. A. Cornell, Science **269**, 198 (1995).
[2] C. C. Bradley, C. A. Sackett, J. J. Tollett, and R. G. Hulet, Phys. Rev. Lett. **75**, 1687 (1995).
[3] K. B. Davis, M.-O. Mewes, M. R. Andrews, N. J. van Druten, D. S. Durfee, D. M. Kurn, and W. Ketterle, Phys. Rev. Lett. **75**, 3969 (1995).

[4] C. A. Condat and R. A. Guyer, Phys. Rev. B **24**, 2874 (1981); D. A. Huse and E. D. Siggia, J. Low Temp. Phys. **46**, 137 (1982); R. V. E. Lovelace and T. J. Tomilla, Phys. Rev. A **35**, 3597 (1987); P. A. Ruprecht, M. J. Holland, K. Burnett, and M. Edwards, Phys. Rev. A **51**, 4704 (1995); M. Lewenstein and L. You, Phys. Rev. A **53**, 909 (1996).

[5] M. Edwards, P. A. Ruprecht, K. Burnett, R. J. Dodd, and C. W. Clark, Phys. Rev. Lett. **77**, 1671 (1996); D. S. Jin, J. R. Ensher, M. R. Matthews, C. E. Wieman, and E. A. Cornell, Phys. Rev. Lett. **77**, 420 (1996); M.-O. Mewes, M. R. Andrews, N. J. van Druten, D. M. Kurn, D. S. Durfee, C. G. Townsend, and W. Ketterle, Phys. Rev. Lett. **77**, 988 (1996); S. Giorgini, L. P. Pitaevskii, and S. Stringari (to be published).

[6] F. Dalfovo and S. Stringari, Phys. Rev. A **53**, 2477 (1996).

[7] M. Holland and J. Cooper, Phys. Rev. A **53**, R1954 (1996); G. Baym and C. Pethick, Phys. Rev. Lett. **76**, 6 (1996).

[8] L. You and M. Holland, Phys. Rev. A **53**, R1 (1996).

[9] W. H. Press *et al.*, *Numerical Recipes in C* (Cambridge University Press, Cambridge, England, 1988).

[10] D. Heinzen (private communication).

[11] Preliminary data were presented by D. S. Jin, J. R. Ensher, M. R. Matthews, C. E. Wieman, and E. A. Cornell, in *Proceedings of the XXI International Conference on Low Temperature Physics, Prague, Czechoslovakia* [Czech. J. Phys. (to be published)]; strong interactions are discussed in M.-O. Mewes *et al.*, Phys. Rev. Lett. **77**, 416 (1996).